Journal of Marine Research, 69, 779–795, 2011

Thermohaline convection at density ratios below one: A new regime for salt fingers

by Raymond W. Schmitt[1]

ABSTRACT

New experimental results on haline convection show a surprising preference for narrow fingers over large-scale convection when even a small stabilizing temperature gradient is present (Hage and Tilgner, 2010). This regime has heat/salt density ratios below one, a parameter range that has not been explored in traditional salt finger theory. Here the properties of the exact (long finger) solutions of Schmitt (1979, 1983) are explored at low density ratios. It is found that narrow finger solutions are indeed obtained and remain the fastest growing in some circumstances, though the selective advantage of the "Stern scale" can disappear as the density ratio decreases. The variation of solutions with Prandtl number and the relation to the Stern (1975) approximate solution are examined and discussed.

1. Introduction

Stern (1960) introduced the world to salt fingers and initiated study into the various forms of double-diffusive convection. Over the years he contributed much to the intellectual advance of this new branch of fluid mechanics. Interest in salt fingers is now reviving since direct tracer release experiments have shown the vertical fluxes in fingering staircases to be large (Schmitt *et al.*, 2005; Veronis, 2007), and evidence supporting the hypothesized (Schmitt, 1981, 1990) effects of fingers on the thermohaline stratification is emerging in the ARGO profiling float data set (Johnson, 2006). Indeed, Johnson and Kearney (2009) find that fingers have attenuated the signals of climate change in the thermocline. Discussions of various aspects of double-diffusion have been provided by a collection of reviews introduced by Ruddick and Gargett (2003), including work on salt fingers (Kunze, 2003; Schmitt, 2003; Yoshida and Nagashima, 2003a) diffusive-convection (Kelley *et al.*., 2003) and double-diffusive intrusions (Ruddick and Kerr, 2003; Ruddick and Richards, 2003; Ruddick, 2003; Yoshida and Nagashima, 2003b). Stern himself continued to make significant contributions to double-diffusive theory throughout his career (Stern *et al.*, 2001). However, our focus here will be on a previously unknown parameter regime for salt fingers revealed by the recent experiments of Hage and Tilgner (2010). We place the discussion in the context of one of Stern's most useful contributions to salt finger theory.

1. Department of Physical Oceanography, Woods Hole Oceanographic Institution, Woods Hole, Massachusetts, 02543, U.S.A. ***email: rschmitt@whoi.edu***

Specifically, Stern (1975) presented a solution to the growing finger problem that applies in a fluid with uniform vertical gradients of temperature and salinity. This theory may have its origin in an "equilibrium" finger model first proposed by W. Malkus (according to Stern, 1969). Stern examined the asymptotic case of large viscosity and small salt diffusivity in his 1975 book and could readily explain the experimental results of Turner (1967) on the heat/salt buoyancy flux ratio of salt fingers. However, at that time, there were new experimental results from the sugar-salt finger system by Lambert and Demenkow (1972) that did not match Stern's asymptotic theory. As a graduate student at the University of Rhode Island at that time, this presented an opportunity for me to more fully explore the long finger solutions, though a significant amount of tedious algebra was required. The complete solutions for all Prandtl number and Lewis number proved quite successful in explaining the differences between heat-salt and salt-sugar fingers (Schmitt, 1979, 1983). Stern's asymptotic theory continues to be rediscovered by later generations of researchers (Kunze, 1987; Smyth and Kimura, 2007), perhaps indicating that books are not the best repositories for original contributions.

In the following, the properties of the exact long finger solutions in the "density ratio less than one" regime are explored. This is a regime where narrow fingers were not thought to be dominant. Here the salt gradient is strongly destabilizing and the temperature gradient is only weakly stabilizing. The work is motivated by surprising recent experimental results on haline convection by Hage and Tilgner (2010). Pure haline-driven convection is not easily explored in the laboratory; osmotic membranes would seem to be necessary. Hage and Tilgner used an electro-deposition cell in which copper ions are plated out from one solid copper horizontal plate to another at the top/bottom of the cell. To quote their abstract: "An electrodeposition cell is used to sustain a destabilizing concentration difference of copper ions in aqueous solution between the top and bottom boundaries of the cell. The resulting convecting motion is analogous to Rayleigh–Bénard convection at high Prandtl numbers. In addition, a stabilizing temperature gradient is imposed across the cell. Even for thermal buoyancy two orders of magnitude smaller than chemical buoyancy, the presence of the weak stabilizing gradient has a profound effect on the convection pattern. Double diffusive fingers appear in all cases."

Figures 1 and 2 are from Hage and Tilgner (2010). In Figure 1 the red vectors represent velocities measured by particle imaging velocimetry (PIV); the light/dark pattern represents the intensity of the up- (light) or down-going (dark) fluid velocities. The right panel shows the expected large scale "salt" convection when the plates are held at the same temperature, the left panel shows narrow finger cells when a very slight stable temperature gradient is imposed. Figure 2 is a shadowgraph of fingering in the salt-convection apparatus. The basic molecular parameters in these experiments are similar to the oceanic heat-salt system, with Prandtl number $\sim$10 and heat/salt diffusivity ratio $\sim$100. The overall density ratio applied at the boundaries is significantly less than one ($\sim 10^{-2}$) in their experiments.

These are very surprising results. It has generally been assumed that haline-driven convection with density ratios below one would be dominated by traditional large-scale convective

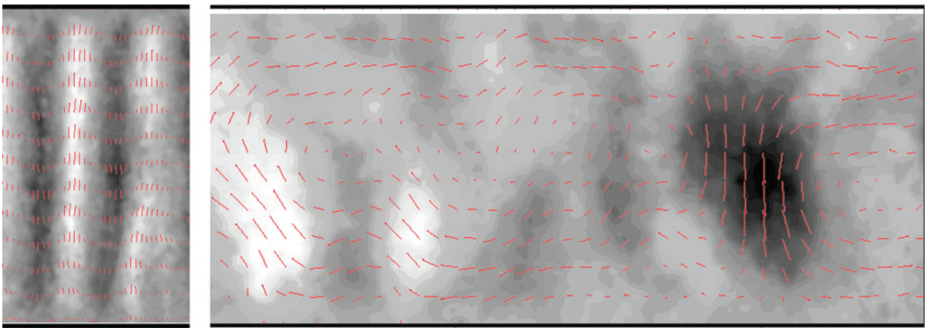

Figure 1. PIV patterns in the experiments of Hage and Tilgner (2010). The images show the entire cell height of 20 mm and extend over a width of 12 mm on the left and 45 mm on the right. The red lines are velocity vectors and the shade of gray indicates the vertical component of velocity (dark = downward, light = upward). The right panel shows large scale convection in the absence of any vertical temperature gradient, the left panel shows narrow fingers when a slight stable temperature gradient is imposed across the cell.

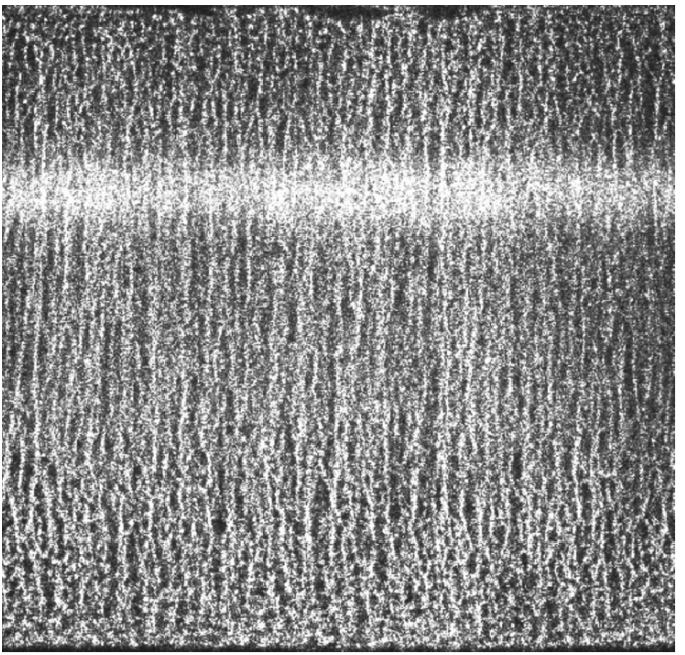

Figure 2. Shadowgraph image from the experiments of Hage and Tilgner (2010). The cell is 80-cm high and 85-cm wide. The bright horizontal bar is an artifact of the illumination. An electric current between copper plates at the top and bottom supplies a destabilizing vertical flux of copper ions across the cell. Narrow fingers appear when a very slight stable vertical temperature gradient is applied.

overturning. These are cells with an order one aspect ratio, with width comparable to layer depth. The large-scale gradients are unstable so there seemed no reason to suspect small-scale fingers would play a role. In addition, the Stern (1975) asymptotic theory predicts a transition to large scales at a density ratio of one, so no one has explored the basic theory in this regime. In the following, the complete solutions of Schmitt (1979, 1983) are examined in the $R_\rho < 1$ parameter range.

2. The long finger solutions

The regime we examine is an unbounded one with uniform gradients of temperature (T) and salinity (S). In the interior of such a linearly stratified fluid, it is possible to describe a field of purely vertical finger motions (elevator modes) that remains valid at finite amplitude, because all the flows are parallel and the gradients of T and S are uniform. The heat and salt equations reduce to a balance between growth, vertical advection and horizontal diffusion (with $\nabla_2^2 =$ horizontal Laplacian):

$$\frac{\partial T}{\partial t} + w\overline{T}_Z = \kappa_T \nabla_2^2 T$$
$$\frac{\partial S}{\partial t} + w\overline{S}_Z = \kappa_S \nabla_2^2 S. \tag{2.1}$$

The momentum balance is between viscous drag and gravitational driving and is given by:

$$\frac{\partial w}{\partial t} = g(\alpha T - \beta S) + \nu \nabla_2^2 w \tag{2.2}$$

$$\text{where } \alpha \equiv -\frac{\partial \rho}{\rho \partial T}, \text{ and } \beta \equiv \frac{\partial \rho}{\rho \partial S}. \tag{2.3}$$

We assume that a mean hydrostatic balance describes the pressure field and that no horizontal motions are associated with the initial growth of the vertical fingers. The exact solutions to the foregoing equations are the mean fields:

$$\overline{T} = T_0 + (z - z_0)\overline{T}_Z$$
$$\overline{S} = S_0 + (z - z_0)\overline{S}_Z \tag{2.4}$$

and finger perturbations:

$$T', S', w' = (\hat{T}, \hat{S}, \hat{w}) \exp(\lambda t) \sin(kx) \sin(ky). \tag{2.5}$$

Here λ is the exponential growth rate of the fingers, k is their horizontal wavenumber and the $\hat{}$ represent "seed" amplitudes for the initial finger growth. Here we have used $\sin(kx)\sin(ky)$ as a simple solution to the Helmholtz equation ($\nabla^2\phi + k^2\phi = 0$) that yields square packed fingers, a planform that is observed in the later stages of laboratory experiments (Williams, 1975). Schmitt (1994a) has shown that a rich variety of finger

planforms are available to satisfy the Helmholtz equation, but this has no impact on the essential relation between growth and the total horizontal wavenumber.

The growth rate depends on several nondimensional parameters as well as the wavenumber (and flux ratio) of the fingers. There are two constants involving the diffusivities of heat, salt and momentum, the Prandtl number, $Pr = \frac{\nu}{\kappa_T}$ and the diffusivity ratio or Lewis number, $Le = \frac{\kappa_T}{\kappa_S}$. For seawater, and the Hage and Tilgner experiments, the Prandtl number is ~7–10 and the Lewis number ~100. The main environmental parameter is the density ratio R_ρ, given by:

$$R_\rho \equiv \frac{\alpha \overline{T}_Z}{\beta \overline{S}_Z}. \tag{2.6}$$

This expresses the degree to which the temperature gradient over-stabilizes the adverse salinity gradient; values much greater than one representing more stable water than those situations with near neutral stability ($R_\rho = 1$), where fingers can grow most rapidly. For much of the subtropical thermocline, R_ρ tends to be near 2, indicating a strong propensity for salt fingering. The maximum density ratio at which fingers can grow is just the Lewis number (~100), since at that value the salinity gradient is too weak to overcome the damping effects of salt diffusion.

An important derived parameter for salt fingers is the ratio of the thermal buoyancy flux to the haline buoyancy flux. The flux ratio (γ) is defined as:

$$\gamma = \frac{\overline{w'\alpha T'}}{\overline{w'\beta S'}}. \tag{2.7}$$

For any given wavenumber it can also be defined by the ratio of the thermal and haline density anomalies:

$$\gamma = \frac{\alpha T'(k)}{\beta S'(k)} \tag{2.8}$$

which is very useful for understanding salt finger dynamics. That is, we expect a wide finger to retain a larger thermal anomaly due to reduced diffusion, while very narrow fingers would have a lower flux ratio due to the enhanced short circuiting of heat between up- and downgoing fingers.

Thus, a close connection between flux ratio and wave number is expected. We also note that energetics places an upward limit on the value of the flux ratio of 1.0, since no more buoyancy can be gained by the heat field than is extracted from the salt distribution. By setting the time derivative to zero in Eqs. (2.1–2.3), we can examine the properties of the "equilibrium finger", in which heat and salt diffusion just balance each other, and find that the lower limit of flux ratio at a given density ratio is just:

$$\gamma_{eq} = \frac{\kappa_S \alpha \overline{T}_Z}{\kappa_T \beta \overline{S}_Z} = \frac{R_\rho}{Le} \tag{2.9}$$

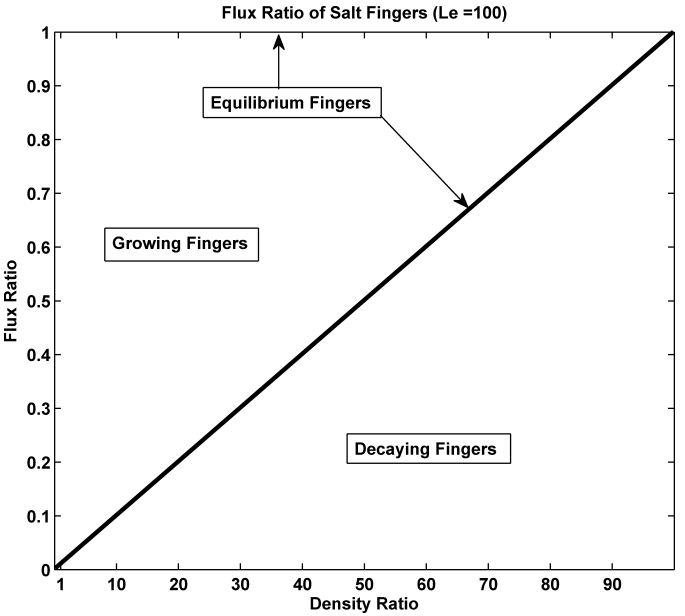

Figure 3. Flux ratio versus density ratio space for heat-salt fingers. Energetics sets an upper limit of $\gamma = 1$, where heat and salt anomalies cancel and there is no density anomaly to drive the fingers. Salt diffusion sets a lower limit of $\gamma = R_\rho/Le$ where narrow fingers diffuse enough salt to yield zero growth rate. No fingers can form in a uniform gradient region for $R_\rho > Le$ ($\sim$100 for heat – salt).

Thus, at low R_ρ a wide range of fingers can grow, but when $R_\rho \to Le$ only fingers with a flux ratio near one can exist. This limited range of allowable flux ratios and wavenumbers is the likely explanation for the increasing order displayed in finger planforms as experiments run down and the density ratio approaches its upward limit and one wavenumber comes to dominate the field (Williams, 1975). Strongly forced fingers at low density ratios are much more irregular in appearance, and numerical simulations display increasingly chaotic and turbulent appearing structures as $R_\rho \to 1$.

It is useful to examine these issues in a plot of flux ratio against density ratio (Fig. 3). Values of flux ratio above the diagonal line (Eq 2.9) represent growing fingers; those below are decaying fingers. The equilibrium finger with the $\lambda = 0$ ($\gamma = R_\rho/Le$) line separates the two domains.

While the no-growth lines can be identified by inspection of the equations, finding the maximum growth rate requires some algebra. Schmitt (1979, 1983) has provided solutions for the scaled growth rate and wavenumber as functions of the flux ratio:

$$G = \frac{\lambda}{(g\alpha\overline{T}_z)^{1/2}} \tag{2.10}$$

$$K = \frac{k}{\left(\frac{g\alpha\overline{T}_z}{\nu\kappa_T}\right)^{1/4}} \tag{2.11}$$

$$G = (Le\gamma - R_\rho)\left\{\frac{(1-\gamma)}{\gamma R_\rho(Le-1)[R_\rho(PrLe-1) - Le\gamma(Pr-1)]}\right\}^{1/2} \tag{2.12}$$

$$K = (R_\rho - \gamma)^{1/2} Le^{1/2}\left\{\frac{Pr(1-\gamma)}{\gamma R_\rho(Le-1)[R_\rho(PrLe-1) - Le\gamma(Pr-1)]}\right\}^{1/4}. \tag{2.13}$$

These relations have been explored for the purposes of finger spectra (Gargett and Schmitt, 1982; Shen and Schmitt, 1996) and the flux ratio. In particular, the flux ratio of the fastest growing finger has proven to be a good predictor of the flux ratio realized in both the heat-salt and salt-sugar experimental regimes (Fig. 4).

The ability of the exact solutions to predict the variation of flux ratio with Lewis number, Prandtl number and to some extent density ratio, provided great impetus for its further application to the problem of the salt finger width, at which it also succeeded (Gargett and Schmitt, 1982; Marmorino *et al.*, 1987). Oceanic observations of the finger width are quite consistent with the "Stern scale" of $\sim 2\pi(g\alpha T_Z/\nu\kappa_T)^{-1/4}$, which is typically a few centimeters. St Laurent and Schmitt (1999) showed how oceanic data on thermal and kinetic energy dissipation in the salt finger regime implies a fall-off in flux ratio with increasing density ratio, similar to the theory at density ratios from 1–4. To date no data have been produced to show an increase in flux ratio with even higher density ratios but such behavior is a key feature of the layering instabilities discussed by Radko (2003, 2005, 2007) so would be of interest. It is easy to argue that an increase in flux ratio with increasing density ratio is sure to occur in the ocean by the dominance of turbulence at higher density ratios, where finger growth rates are small.

The fastest growing finger curves of Figure 4 are obtained by maximizing the expression for G with respect to flux ratio; that is, $\partial G/\partial\gamma = 0$, yielding a cubic in γ: $a\gamma^3 + b\gamma^2 + c\gamma + d = 0$. With

$$a = (Pr-1),\ b = (Pr+1-2PrLe)\frac{R_\rho}{Le},\ c = (PrLe+1-2Pr),\ d = (PrLe-1)\frac{R_\rho^2}{Le^2},$$

$$H = \frac{(b^2-3ac)}{9a^2},\ J = \frac{(2b^3-9abc+27a^2d)}{27a^3},\ and\ \theta = \frac{1}{3}\arccos\left[\frac{-J}{2H^{3/2}}\right] \tag{2.14}$$

the solutions for the growth maximizing flux ratio (γ_m) are defined in different Prandtl number regimes:

$$Pr = 0, \quad \gamma_m = \left[\frac{R_\rho}{Le}\right]^{\frac{1}{2}}$$

$$Pr < 1, \quad \gamma_m = 2H^{\frac{1}{2}}\cos(\theta) - \frac{b}{3a}$$

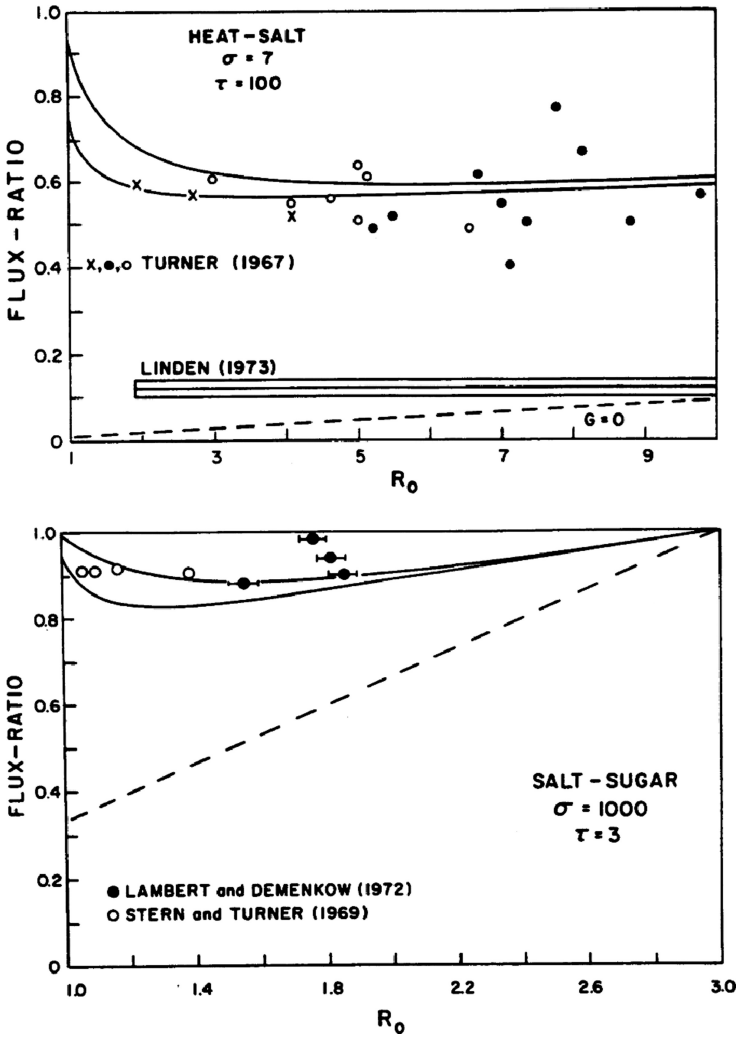

Figure 4. Flux ratio from laboratory data compared with the flux ratio of the fastest growing finger (solid curves) in the heat-salt (top) and salt-sugar (bottom) regimes. The equilibrium finger with $\lambda = 0$ is shown as a dashed line. From Schmitt (1979).

$$Pr = 1, \quad \gamma_m = \frac{1}{2}\left[\frac{1}{4} + \frac{2R_\rho}{Le}\right]^{\frac{1}{2}} + \frac{1}{4}$$

$$Pr > 1, \quad \gamma_m = 2H^{\frac{1}{2}} \cos\left(\theta + \frac{4\pi}{3}\right) - \frac{b}{3a}. \tag{2.15}$$

The variation of the solutions with Prandtl number is of some interest, and helps us to understand the asymptotic solution of Stern (1975). In our notation, Stern's expression for

the flux ratio of the fastest growing long fingers in the high Prandtl number and Lewis number regime is:

$$\gamma = R_\rho - [R_\rho(R_\rho - 1)]^{1/2}. \tag{2.16}$$

Figures 5a,b compare the Stern asymptotic solution with the full solution. Stern's solution has a flux ratio of one at $R_\rho = 1$, hitting the energetic limit for fingers. However, at $R_\rho = 1$, the full solution of Schmitt has a flux ratio of 0.73 for $Pr = 7$ and $Le = 100$. The "zero wavenumber" limit (Eq. 2.13) is not met until the flux and density ratios equal 0.876 for Pr = 7 and Le = 100. The line represented by $\gamma = R_\rho$ is an advective limit for finger solutions that replaces the energetic limit for $R_\rho < 1$. That is, the line $\gamma = R_\rho$ represents the effects of advection and/or pure vertical turbulence. Heat and salt perturbations in that case are in proportion to their ratio in the background gradients. In this uniform gradient situation, fingers cannot carry a larger temperature perturbation relative to salt than is available in the background gradients. When the flux ratio of the fastest growing finger merges with the $\gamma = R_\rho$ line for $R_\rho < 1$, then Eq. 2.13 indicates that the horizontal wavenumber goes to zero and the convection cells should be large. In the high Prandtl number limit examined by Stern (1975) this happens at $R_\rho = 1$. Both the energetic and advective limits are reached at the same point. However, the full solutions of Schmitt (1979, 1983) show that a narrow "Stern scale" finger can still be the fastest growing at $R_\rho = 1$ and below. The zero wavenumber limit for the fastest growing fingers is not met until $\gamma_m = R_\rho$ for finite Prandtl number. Of course, slower growing fingers with a narrow width are possible anywhere in the $\gamma < R_\rho$, $R_\rho < 1$ wedge.

Further exploration of this new parameter range suggests a reconsideration of the growth rate scaling introduced in Eq. 2.10. Since we are exploring a regime where the temperature gradient becomes very small, the traditional scaling of growth rate with temperature gradient may be deemed inappropriate. (It remains the scaling of choice in the oceanic thermocline, as the temperature gradient is always much easier to measure than the salinity gradient.) That is, with the vertical temperature gradient becoming small as $R_\rho \to 0$, there will be an "artificial" increase in nondimensional growth rate in that limit. In this $R_\rho < 1$ and $T_z \to 0$ regime, it is appropriate to scale with the vertical salinity gradient. Kunze (1987) used this scaling in his analysis. Here this is easily done with a factor of $R_\rho^{1/2}$ applied to Eq. 2.10. That is:

$$G_S = \frac{\lambda}{(g\beta S_Z)^{1/2}} = R_\rho^{1/2} G. \tag{2.17}$$

The two different growth rate scalings are contrasted in Figure 6.

Similarly, we expect that the wavenumber scaling based on temperature gradient will become problematic as the temperature gradient vanishes for $R_\rho \to 0$. The nondimensional wavenumber scaled with the salinity gradient is given by:

$$K_S = \frac{k}{\left(\frac{g\beta \overline{S}_Z}{\nu \kappa_T}\right)^{1/4}} = R_\rho^{1/4} K. \tag{2.18}$$

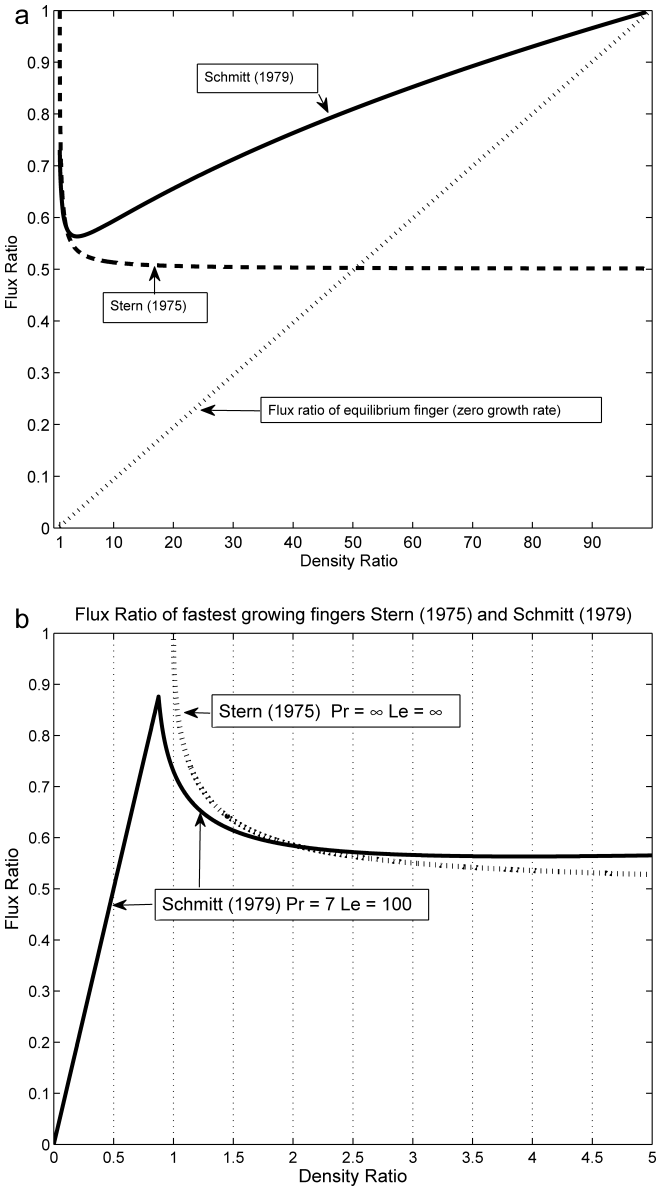

Figure 5. (a) Flux ratio as a function of density ratio for the fastest growing fingers of Stern (1975) (dashed), and for Schmitt (1979) (solid). The flux ratio of the nongrowing "equilibrium" finger where thermal and salt diffusion are in balance, is shown as a dotted line. (b) Detailed behavior of the flux ratio in the finger solutions of Stern (1975) (dashed) and Schmitt (1979) (solid) at low R_ρ. Stern's asymptotic solution reaches the upper (energy) limit of $\gamma = 1$ at $R_\rho = 1$, but the flux ratio of the full solution of Schmitt remains below one for heat-salt fingers even for density ratios less than one. Solutions are limited at $R_\rho < 0.876$ by an advective constraint, where $\gamma = R_\rho$ and the wavenumber goes to zero (Eq. 2.13).

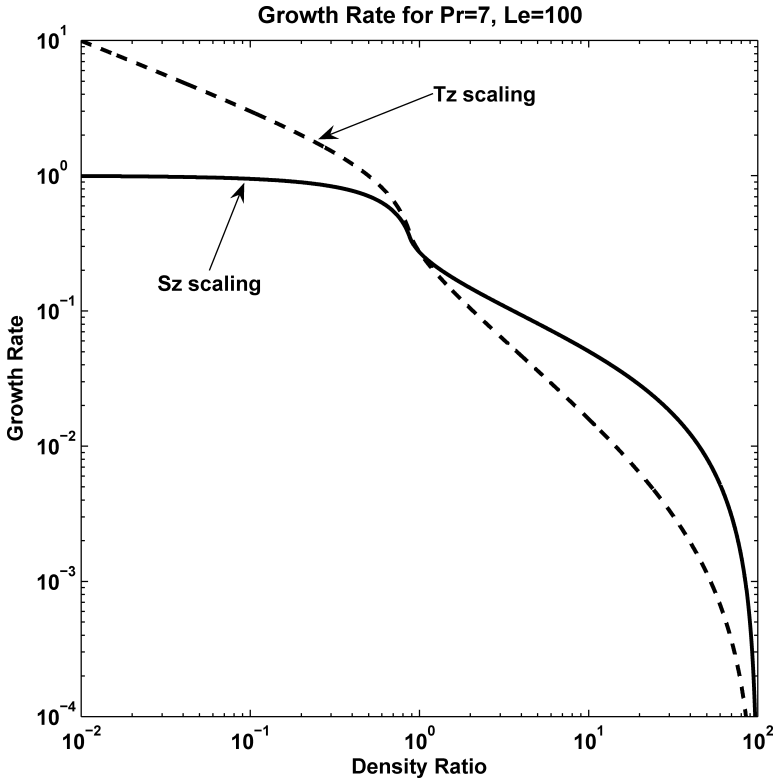

Figure 6. Log-log comparison of the nondimensional temperature and salinity growth rate scalings for heat-salt fingers. Note that the maximum growth rate with salinity gradient scaling approaches a constant of one as R_ρ gets small.

As in Gargett and Schmitt (1982), we can examine the growth rate as a function of wavenumber for several different density ratios in order to understand the expected horizontal spectra for fingers, using the salinity gradient scalings (Fig. 7a,b). The basic "Stern wavenumber" given by $K \sim 1$ for the fastest growing finger is seen to dominate the finger spectra in the usual $R_\rho > 1$ regime, but loses its selective advantage entirely at $R_\rho = 1$ in the large Prandtl number limit of Stern (Fig. 7a), where the (wide) (zero wavenumber) fingers have the fastest growth. In contrast, for the Schmitt (1979, 1983) solutions (Fig. 7b) a growth rate advantage for the Stern-scale finger persists to a density ratio of 0.876 for the heat-salt system of $Pr = 7$, $Le = 100$. At lower density ratios the growth rate peak vanishes and all low wavenumber fingers grow equally well.

The existence of spectral peaks at low density ratios is a function of the Prandtl number. Additional growth rate 'spectra' are shown in Figure 8a,b for Prandtl numbers of 1 and 0.1. The lower the Prandtl number the lower the density ratio where the advective limit is reached

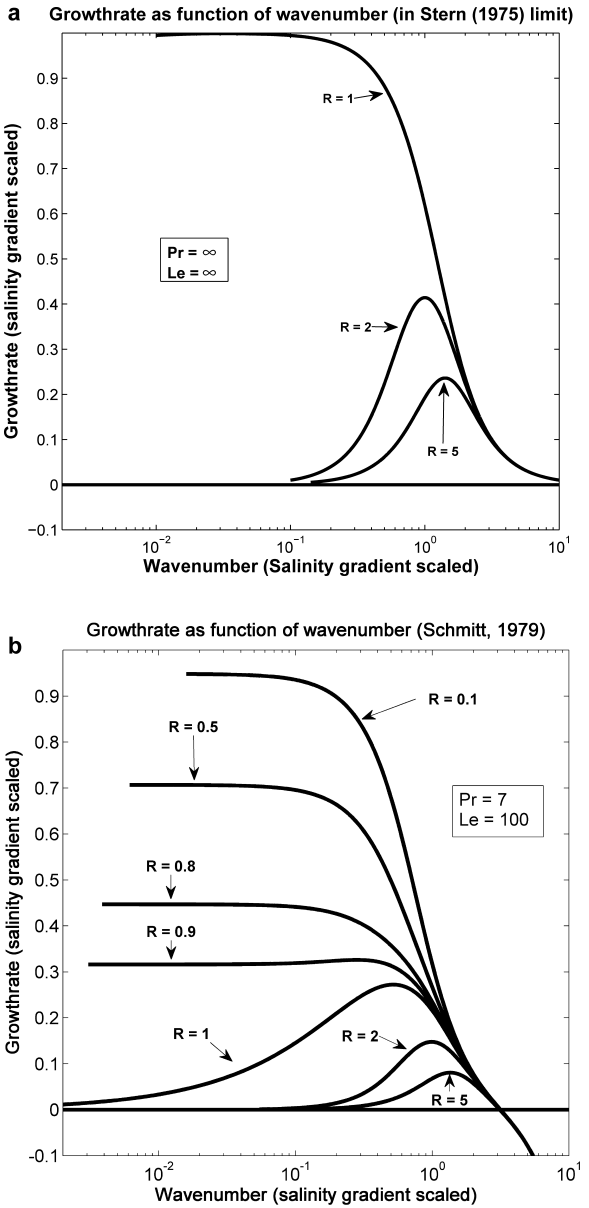

Figure 7. (a) Growth rate as a function of finger wavenumber in the Stern limit of large Prandtl and Lewis numbers for $R_\rho = 1, 2, 5$. The growth rate and wavenumber have been scaled with the salinity gradient and renormalized to compensate for a $Pr^{-1/2}$ dependence of growth rate (See Eq. 5 of Schmitt, 1994b). Note that growth remains positive even for high wavenumber fingers because there is no salt diffusion. (b) Growth rate as a function of wavenumber for $Pr = 7$ and $Le = 100$ for the finger solutions of Schmitt (1979, 1983) for various R_ρ. High wavenumber fingers are damped by salt diffusion. A fastest growing "Stern scale" finger persists to a density ratio of 0.876 for $Pr = 7$ and $Le = 100$. At lower R_ρ the growth rate advantage vanishes, and the spectrum become white at low wavenumbers.

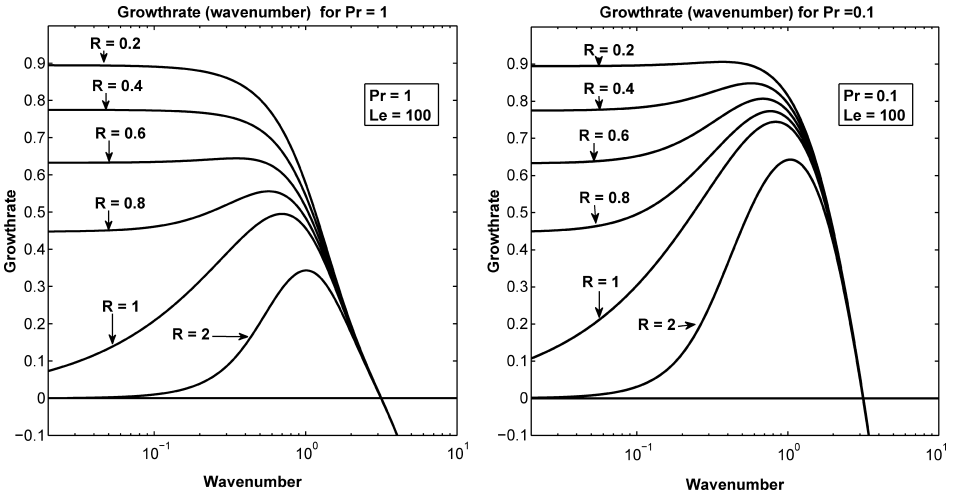

Figure 8. (a) (left) Growth rate as a function of wavenumber for various R_ρ with $Pr = 1$. (b) (right) Growth rate as a function of wavenumber for various R_ρ with $Pr = 0.1$.

and the wavenumber vanishes (Eq. 2.13). For $Pr = 0.1$ there is still a peak growth rate at an order one wavenumber even for $R_\rho = 0.2$, though the growth rate advantage over lower wave numbers is small. For $Pr = 1$ the peak in growth rate vanishes for $R_\rho \sim 0.5$. At density ratios less than this the spectrum transitions to a broad 'white' low wavenumber regime.

Additional insight is gained by examining the flux ratio of the fastest growing fingers as a function of density ratio in log-log space for different Prandtl numbers (Fig. 9). While the fastest growing finger has a high flux ratio at $R_\rho = 1$ for large Prandtl numbers (Stern limit), lower flux ratios are found for smaller Prandtl numbers. The smaller the Prandtl number the smaller the density ratio at which a 'Stern-scale" finger has the fastest growth. Once the flux ratio of maximum growth hits the $\gamma = R_\rho$ advective limit, wider fingers have the fastest growth. In the normal $R_\rho > 1$ regime, the different behavior of the curves suggests that the layer formation and regulation mechanisms of Radko (2003, 2005, 2007) which depend on a minimum flux ratio at an intermediate R_ρ, would not work in low Prandtl number fluids. This is of interest for possible thermohaline layering in stellar interiors.

3. Discussion

The foregoing analysis of the exact long finger solutions of Schmitt (1979, 1983) in the $R_\rho < 1$ regime tells us that: (1) Fast growing, narrow finger solutions do exist in this new regime; (2) For order one Prandtl numbers and density ratios just below one, narrow, Stern-scale fingers can have the fastest growth; (3) The growth rate advantage of the Stern scale fingers expands for low Prandtl number fluids; and (4) The growth rate advantage vanishes for high Prandtl number fluids, as low wavenumber modes have substantial growth rates.

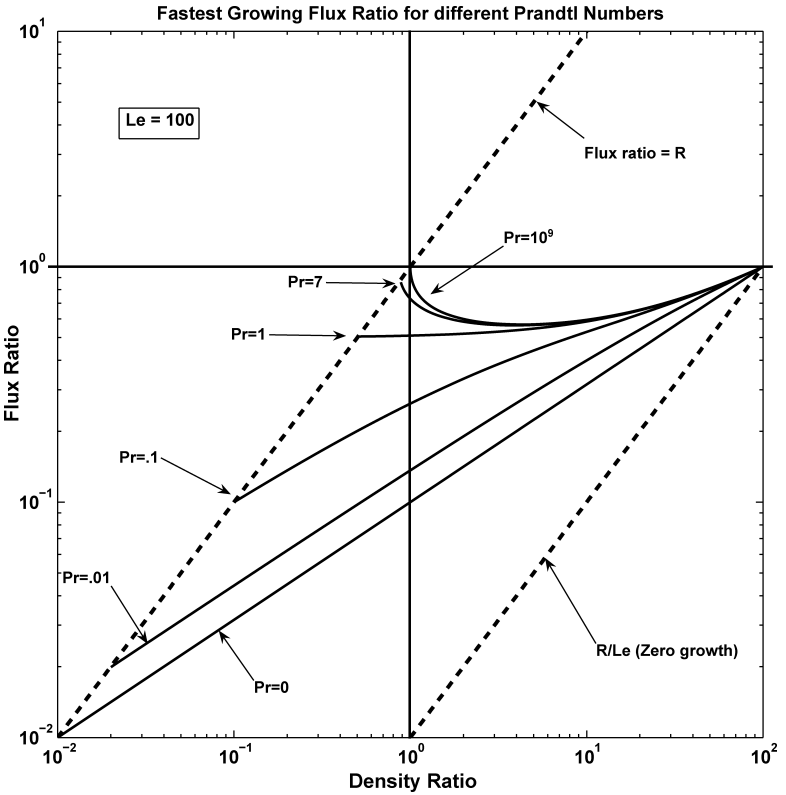

Figure 9. The flux ratio of the fastest growing finger as a function of density ratio for a diffusivity ratio $Le = 100$ and various Prandtl numbers, in log-log space. Once the curves reach the advective limit of $\gamma = R_\rho$, the spectrum becomes white at low wavenumbers, and the growth rate advantage of the Stern-scale fingers is lost to wider fingers.

Thus, while theory certainly allows narrow convective cells, we lack a complete explanation of the new observations of Hage and Tilgner (2010).

It seems likely that an additional factor is at play in these experiments. That is, while the interior solutions yield narrow fingers with substantial growth rates, it is not clear that they should be preferred over wider fingers, except in the case where the density ratio is just below one, and the Hage and Tilgner experiments have a density ratio of order 10^{-2}. It is likely that the rigid top and bottom boundary condition of these experiments is playing a role. There will be thermal and haline diffusive boundary layers at the top and bottom to maintain the heat and salt fluxes in the interior. It will always be true that the salt boundary layer is much thinner than the thermal boundary layer, by a factor of $Le^{-1/2}$ (Linden and Shirtcliffe, 1978). Convection driven by the thin haline boundary layers seems very likely to be providing a narrow, high wavenumber seed spectrum to the interior finger solutions examined here. Since the growth rates for all wavenumbers are substantial at low density

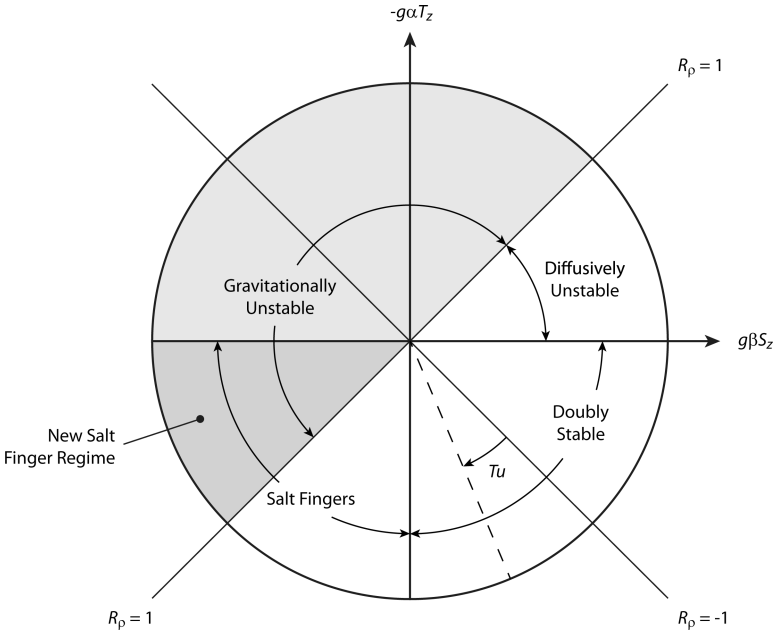

Figure 10. The $T_Z - S_Z$ stability plane with the new fingering regime identified, following Ruddick (1983). The gray colored sector above the $R_\rho = +1$ line is gravitationally unstable, and the indicated wedge (darker gray) shows where the fingers of Hage and Tilgner (2010) would be found. The Turner Angle (Tu) is defined as shown. Its relationship to the slope R_ρ is given by $R_\rho = -\tan(Tu + 45°)$.

ratio, a higher wavenumber boundary layer seed spectrum may be sufficient to produce the observed narrow fingers in the interior.

Another possibility is that the interior temperature and salinity gradients evolve to have a density ratio quite different from that imposed at the boundaries. As noted and illustrated in Schmitt (1979, 1981, 1990), the greater transport of salt than heat will modify the density ratio, tending to increase it in the interior. Any narrow fingers, perhaps seeded by plumes from the thin haline boundary layers, would have a flux ratio below the $\gamma = R_\rho$ line and would thus tend to increase R_ρ, making fingers even more preferred over larger scale convection. It is possible that the interior gradients actually have density ratio greater than one, if the salinity gradient is reduced sufficiently. Thus the bulk of the fluid could actually be supporting "normal" fingers. Some preliminary numerical model runs with $R_\rho < 1$ by T. Radko (pers. comm.) suggest that this is indeed the case. Additional experimental measurements and direct numerical simulations would be very illuminating in determining the operant physics in these experiments.

Finally, we note that the traditional depiction of the limits of salt finger convection in "Turner angle" space (Ruddick, 1983) must now be redrawn. That is, the Hage and Tilgner experiments require us to expand the salt finger sector from 1/8 to 1/4 of the $T_z - S_z$ plane (Fig. 10). Whether this new finger regime plays a significant role in ocean mixing remains

to be seen, but it may be active in the surface mixing layer under evaporative conditions with solar heating and within the mixed layers of thermohaline staircases.

Acknowledgments. The excellent education and generous advice received from Professor Melvin Stern have been a tremendous help to my career. His unique physical insights have provided decades of inspiration for research. The financial support of NASA for this work under grant NNX10AE19G is also gratefully acknowledged.

REFERENCES

Gargett, A. E. and R. W. Schmitt. 1982. Observations of salt fingers in the central waters of the eastern North Pacific. J. Geophys. Res., *87*, C10, 8017–8029.

Hage, E. and A. Tilgner. 2010. High Rayleigh number convection with double diffusive fingers. Phys. Fluids, *22*, 076603-1–7. doi: 10.1063/1.3464158

Johnson, G. C. 2006. Generation and initial evolution of a MODE water $\theta - S$ anomaly. J. Phys. Oceanogr., *36*, 739–751.

Johnson, G. C. and K. A. Kearney. 2009. Ocean climate change fingerprints attenuated by salt fingering? Geophys. Res. Lett. *36*, L21603, doi:10.1029/2009GL04069721.

Kelley, D. E., H. J. S. Fernando, A. E. Gargett, J. Tanny and E. Özsoy. 2003. The diffusive regime of double-diffusive convection. Prog. Oceanogr., *56*, 461–481.

Kunze, E. 1987. Limits on growing finite length salt fingers: A Richardson number constraint. J. Mar. Res., *45*, 533–556.

—— 2003. A review of salt fingering theory. Prog. Oceanogr., *56*, 399–417.

Lambert, R. B. and J. W. Demenkow. 1972. On the vertical transport due to fingers in double diffusive convection. J. Fluid Mech., *54*, 627–640.

Linden, P. E. and T. Shirtcliffe. 1978. The diffusive interface in double-diffusive convection. J. Fluid Mech., *87*, 417–432.

Marmorino, G. O., W. K. Brown, and W. D. Morris. 1987. Two-dimensional temperature structure in the C-SALT thermohaline staircase. Deep-Sea Res., *23*, 1667–1675.

Radko, T. 2003. A mechanism for layer formation in a double-diffusive fluid. J. Fluid Mech., *497*, 365–380.

—— 2005. What determines the thickness of layers in a thermohaline staircase? J. Fluid Mech., *523*, 79–98.

—— 2007. Mechanics of merging events for a series of layers in a stratified turbulent fluid. J. Fluid Mech., *577*, 251–273.

Ruddick, B. 1983. A practical indicator of the stability of the water column to double-diffusive activity. Deep-Sea Res., *30*, 1105–1107.

—— 2003. Laboratory studies of interleaving. Prog. Oceanogr., *56*, 529–547.

Ruddick, B. and A. E. Gargett. 2003. Oceanic double-infusion: Introduction. Prog. Oceanogr., *56*, 381–393.

Ruddick B. R. and O. Kerr. 2003. Oceanic thermohaline intrusions: theory. Prog. Oceanogr., *56*, 483–497.

Ruddick B. R. and K. Richards. 2003. Oceanic thermohaline intrusions: Observations. Prog. Oceanogr., *56*, 499–527.

Schmitt, R. W. 1979. The growth rate of super-critical salt fingers. Deep-Sea Res., *26A*, 23–40.

—— 1981. Form of the temperature-salinity relationship in the Central Water: Evidence for double-diffusive mixing. J. Phys. Oceanogr., *11*, 1015–1026.

—— 1983. The characteristics of salt fingers in a variety of fluid systems, including stellar interiors, liquid metals, oceans, and magmas. Phys. Fluids, *26*, 2373–2377.
—— 1990. On the density ratio balance in the central water. J. Phys. Oceanogr., *20*, 900–906.
—— 1994a. Triangular and asymmetric salt fingers. J. Phys. Oceanogr., *24*, 855–860.
—— 1994b. Double-diffusion in oceanography. Ann. Rev. Fluid Mech., *26*, 255–285.
—— 2003. Observational and laboratory insights into salt finger convection. Prog. Oceanogr., *56*, 419–433.
Schmitt, R. W., J. R. Ledwell, E. T. Montgomery, K. L. Polzin, and J. M. Toole. 2005. Enhanced diapycnal mixing by salt fingers in the thermocline of the tropical Atlantic. Science, *308*, 685–688.
Shen, C. and R. W. Schmitt. 1996. The wavenumber spectrum of salt fingers, *in* Double-Diffusive Convection, A. Brandt and H. Fernando, eds., AGU Geophysical Monograph, *94*, 305–312.
Smyth, W. D. and S. Kimura. 2007. Instability and diapycnal momentum transport in a double-diffusive, stratified shear layer. J. Phys. Oceanogr., *37*, 1551–1565.
Stern, M. E. 1960. The 'salt fountain' and thermohaline convection. Tellus, *12*, 172–175.
—— 1969. Collective instability of salt fingers. J. Fluid Mech., *35*, 209–218.
—— 1975. Ocean Circulation Physics, Academic Press, NY, 246 pp.
Stern M. E., T. Radko and J. Simeonov. 2001. Salt Fingers in an unbounded thermocline. J. Mar. Res., *59*, 355–390.
St. Laurent, L. and R. W. Schmitt. 1999. The contribution of salt fingers to vertical mixing in the North Atlantic Tracer Release Experiment. J. Phys. Oceanogr., *29*, 1404–1424.
Turner, J. S. 1967. Salt fingers across a density interface. Deep-Sea Res., *14*, 599–611.
Veronis, G. 2007. Updated estimate of double-diffusive fluxes in the C-SALT region. Deep-Sea Res. *54*, 831–833.
Williams, A. J. 1975. Images of ocean microstructure. Deep-Sea Res., *22*, 811–829.
Yoshida, J. and H. Nagashima. 2003a. Numerical experiments on salt finger convection. Prog. Oceanogr., *56*, 435–459.
—— 2003b. Numerical experiments on double-diffusive intrusions in the ocean and their relation to laboratory experiments. Prog. Oceanogr., *56*, 549–557.

Received: *18 April, 2011*; revised: *2 September, 2011*.